CHALMERS
UNIVERSITY OF TECHNOLOGY

An Osseointegrated Load Analysis of an Open-Source Active Lower Limb Prosthesis

Master's thesis in Biomedical Engineering

BRETT MUSOLF

DEPARTMENT OF ELECTRICAL ENGINEERING
MASTER'S PROGRAM OF BIOMEDICAL ENGINEERING

CHALMERS UNIVERSITY OF TECHNOLOGY
Gothenburg, Sweden 2021
www.chalmers.se

MASTER'S THESIS IN BIOMEDICAL ENGINEERING 2021

An Osseointegrated Load Analysis of an Open-Source Active Lower Limb Prosthesis

BRETT MUSOLF

Department of Electrical Engineering
CHALMERS UNIVERSITY OF TECHNOLOGY
Göteborg, Sweden 2021

An Osseointegrated Load Analysis of an Open-Source Active Lower Limb Prosthesis
BRETT MUSOLF

Supervisor: Kirstin Ahmed, PhD
Supervisor: Alexander Thesleff, PhD
Examiner: Professor Max Ortiz-Catalan
Master's Thesis 2021
Center for Bionics and Pain Research
Department of Electrical Engineering
Chalmers University of Technology
Chalmersplatsen 4, SE-412 96 Gothenburg
Telephone +46 31 772 1000

An Osseointegrated Load Analysis of an Open-Source Active Lower Limb Prosthesis
BRETT MUSOLF
Department of Electrical Engineering
Chalmers University of Technology

Abstract

The University of Michigan's Open-Source Leg (OSL) is a low-cost prosthetic limb with two actuators (commercial drone motors) simulating knee and ankle joints. With the OSL, researchers can have a universal build platform from which to test and develop from. In testing with transfemoral amputee socket users, the OSL has shown promise in producing biomechanics that reflect intact limb user gait over level ground and up and down slopes. However, the existing joint actuators had a nonideal torque response when users attempted stair ascent and descent. As a solution to this problem, the first part of this thesis upgraded the actuators with a higher torque motor. This required reintegration of the sensor system to work independently from the actuator system.

One patient cohort who may most benefit from the OSL is transfemoral amputees with skeletally anchored amputation prostheses. In contrast to conventional socket users where the soft tissue of the residual limb is loaded, the bone is directly loaded in users with skeletal anchors. This has many advantages but requires a surgery, careful rehabilitation, and a managed loading protocol. To protect the bone throughout this loading regime it is important to understand the forces and moments arising from the OSL and body loads of daily living. The second part of this thesis measured the forces and moments in the exoprosthetic part of the percutaneous implant and used this to assess the safety of the upgraded OSL and make recommendations as to motor torque settings for use of this device in daily life. The results showed kinetic gait contours similar to existing prosthetics but produced larger moments.

KEYWORDS: Gait Analysis, Osseointegration, Lower Limb Prosthesis, Transfemoral Prosthesis, Prosthesis Control, Gait Load Analysis

Table of Contents

List of Figures

Acknowledgements

I would first like to thank the Center for Bionics and Pain Research (formerly the Biomechatronics and Neurorehabilitation Laboratory) for providing funding and access to development equipment without which this project would have been impossible.

I would like to recognize my first advisor Dr. Alex Thesleff. While attending to his own thesis defense he was still able to provide assistance to me in the initial stages of this project. His support was vital in dealing with the severe problems encountered in doing an international project in a time of global lock downs and travel restrictions.

I would also like to recognize my second advisor Dr. Kirstin Ahmed in guiding me through the process of ordering, constructing, and testing the OSL. With the onslaught of delays and setbacks in this project, she provided a stalwart guide for the direction of this project. This has been a very time consuming process and I am grateful for her commitment.

At the Shirley Ryan AbilityLab in Chicago, I would like to thank my two contacts for mechanical and control: Chandler Clark and Minjae Kim, respectively. They provided data and information that was essential in translating this project into its final form.

I would like to thank Truong Tat Nhat Minh and Kurt Stewart for their technical insights that helped expediate the work on this project.

Lastly, I would like to thank Jenna Anderson for her facilitation of work during crucial periods of development of this project.

Introduction

A Global Problem

The loss of a lower limb is a life redefining experience, which can result in sudden and dramatic changes that impact the simplest of daily life tasks. Tasks such as standing, and walking are no longer practical without assistance. In Sweden, there were 33 - 39 lower limb amputations per every 100,000 inhabitants from 1998-2016 resulting from diabetes, dysvascular diseases and trauma [1]. Lower limb prostheses can support amputations at the transfemoral (47%) or transtibial level (26%). There are many commercially available prosthetic options for both and many more in development.

Despite increasing availability and sophistication of prostheses, many users still do not regularly wear their prosthesis. More than 10% of transfemoral amputees use their prosthesis for less than 6 hours a day [2] as a result of discomfort or lack of perceived prosthetic benefit [3]. Discomfort arises from prosthetic socket compression on the user's residual limb which can lead to recurrent skin infections, soft tissue scarring and several more issues leading to poor socket retention. An alternative is directly mounting the prosthesis to the bone of the residual limb through osseointegration (bone ingrowth).

The Diversity of Lower Limb Prosthetics

Prosthetic lower limb features can be divided into two different elements of the prosthesis: the propulsion systems and the support systems (Figure 1).

Propulsion

The most basic propulsion system, a passive prosthesis, provides the user a device to support themselves on. These prostheses allow the users freedom from being wheelchair bound

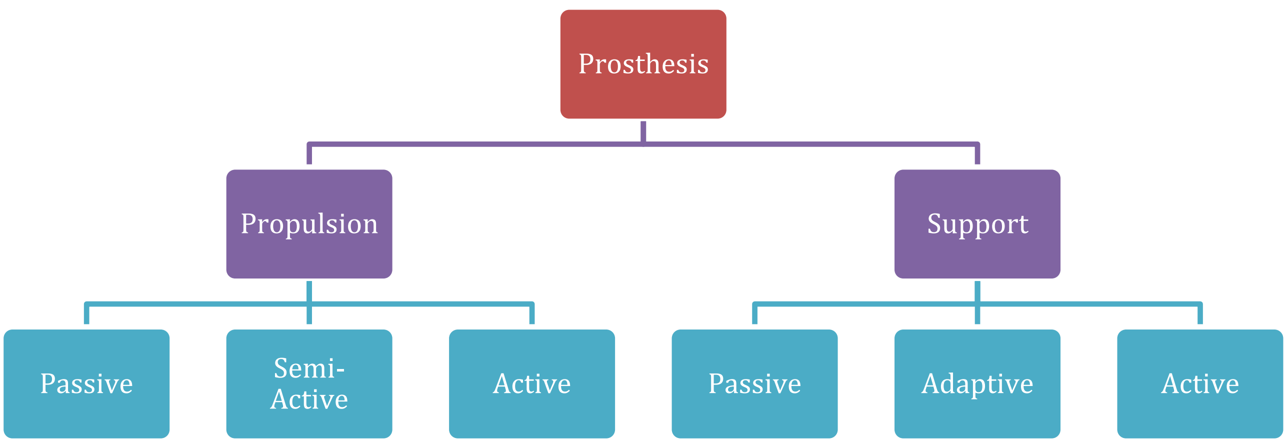

Figure 1. Prosthetic lower limb subdivisions

Figure 2. Examples of passive prosthesis. "Antique Prosthetic Legs" by Curious Expeditions is licensed under CC BY-NC-SA 2.0

and provide an adequate device to stand on. In motion, however, users are obligated to use the remainder of their body to compensate for their missing limb due to the loss of plantarflexion and therefore their primary means of propulsion [4]. More generally, amputees experience asymmetric muscle compensations, increased metabolic cost of walking, reduced preferred speed of gait and large loadings in their sound limb as a result of prosthetic motion deficits [4].

More modern passive prostheses use elastic materials for energy storage and release (ESR) throughout the gait (Figure 3**Error! Reference source not found.**) [5]. Some prostheses

Figure 3. Examples of ESR prostheses [5]. On the right is a conventional prosthesis that uses material and shape energy storage and release. On the left is a prosthesis using a novel linkage system for more efficient storage and release Licensed under CC BY 4.0

integrate motorized clutches or pneumatic cylinders to maximize ESR; these are “semi-active” prostheses.

A third class of prostheses that injects energy into the gait are called “active” prostheses. They are usually driven by electromechanical motors, but novel systems using pneumatic and hydraulics are also being developed [6], [7]. Active prosthetics are intended to generate a ‘joint’ torque that mimics a biological joint. For active knees, this is most distinct in ramp and stair ascents where net positive work is required [8]. For active ankles, providing push off power (plantar flexion) reduces the overall metabolic cost in walking as a result of the reduction in compensatory movements [9], [10].

Support

Support systems can be divided into three categories: passive, adaptive, active [4]. Passive support systems can be from being rigid or have mechanical or fluidic damping systems to illicit a specific response. Adaptive systems control the prosthesis by using a computer and sensors

Figure 4. An adaptive and active prosthetic knee [11]. The Össur Rheo Knee II (on the left) provides adaptive magnetorheological damping to control system response. The Össur Power Knee offers active motion to control system response.

to control resistance to motion [11]. Lastly, active support systems use a motor to regulate motion and position for example the Össur Rheo II and the Össur Power Knee (Figure 4).

State-of-The-Art

A "state-of-the-art" prosthesis in this study is define as having all the following:

1. ***An active propulsion system***
2. ***An active support system***
3. ***Both a knee and the ankle having requirements 1 and 2.***

There exists two commercially available active prosthetics, one being an active knee (the Össur Power Knee [11], [12]) and the other being an active ankle (the Ottobock Empower Ankle [13], [14]). Within developmental research there are a number of projects that offer both an active knee and an active ankle [15]–[20], for example the Open-Source Leg (OSL).

The Open-Source Leg: An Active Knee-ankle Prosthesis

The OSL offers a universal build platform for all researchers [21]. Through this model, researchers can directly compare biomechanical data collected in a controlled way (no other

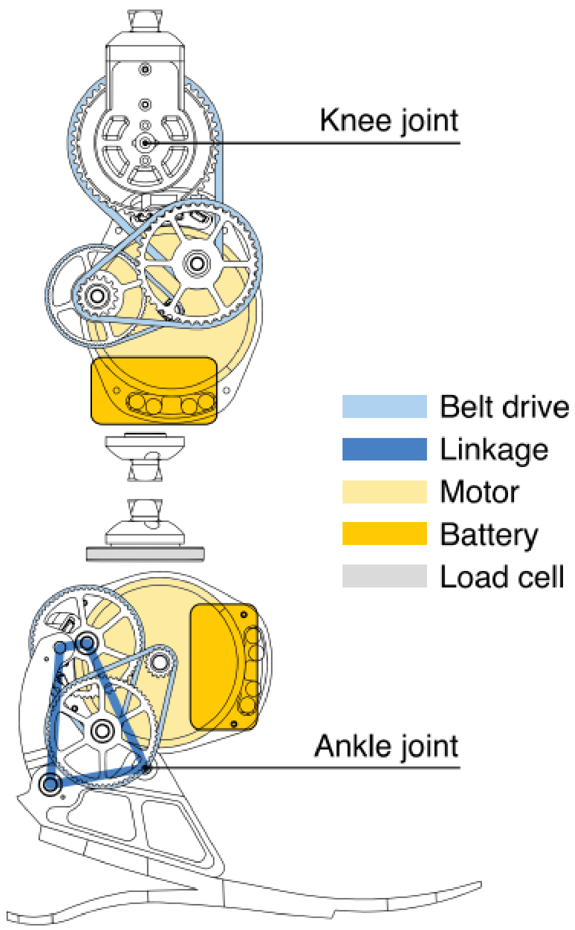

Figure 5. OSL internal layout. Licensed under CC BY 4.0 [20]

variables changed). The cost of ordering and constructing the prosthesis amounts to between 10% – 33% of the equivalent commercial prosthesis.

The OSL in this Study

The data collected in this study used the Shirley Ryan AbilityLab OSL control scheme. The hardware was changed from Dephy motors to Tmotor motors to actuate the knee and ankle joints. This was because the original motors did not offer satisfactory torque for stair climbing. The Dephy motor had a built in IMU, however the Tmotor did not include and IMU, and so these

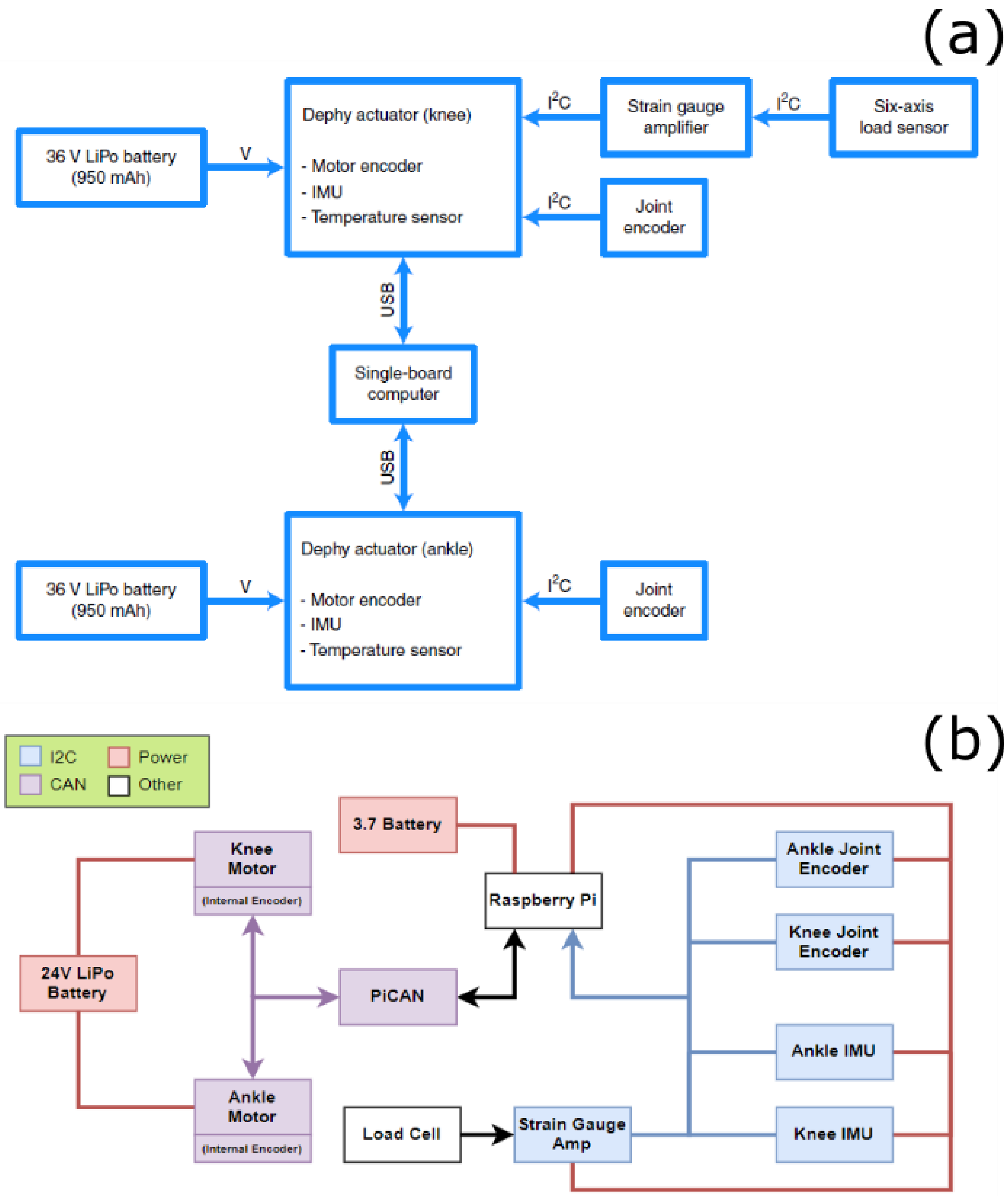

Figure 6. (a) The old OSL schematic. Licensed under CC BY 4.0 [20] (b) and the new schematic.

Table I. Torque values ratios against human requirements. Note that the ankle gearbox varies depending its position. The continuous and instantaneous values were calculated off the continuous and peak motor currents for the Dephy motor and rated and peak torque for the Tmotor motor. A transmission efficiency of 73% was used in these calculations. Average human values used a maximum torque for a 75 kg, 1.7 m individual in level ground or stair ascent/descent [20].

Motor	Joint	Torque (Nm)			
		Continuous		Instantaneous	
		Low	High	Low	High
Dephy	Ankle	0.41	0.72	1.23	2.16
	Knee	0.56	-	7.15	-
Tmotor	Ankle	3.07	5.40	6.13	10.80
	Knee	3.58	-	7.15	-

were mounted externally. The Dephy motor also used I^2C communication along with all other sensors and the communication was managed all within the motor controller which would in turn communicate with the microcontroller. The Tmotor motor, however, could not manage the sensors internally. Therefore, all sensors were managed directly by the microcontroller (as seen in Figure 6). In addition, the Tmotor motors used CAN BUS communication, but all other devices remained in I^2C communication. Therefore, two communications would simultaneously be used in the single system.

Torque Requirements

The impetus for the motor replacement was the non-ideal torque output of the Dephy motor. While it was able to meet the requirements of ambulation, it was reaching these values above its continuous torque range. Table I, shows the Dephy motor close to its instantaneous limit in the ankle at its lower transmission ratio values. In bench testing the temperature of the motor was noted as high while running below the continuous peak. Looking at the torque requirements in ambulation, we see that the Dephy motor would be operating well above the continuous torque rating [20]. The temperature output would therefore be expected to be even higher in prolonged ambulation [22]. Given the values in Table I are assuming a 75 kg, 1.7 m individual, these limits would also have a greater impact on the prosthesis' capabilities when a larger individual uses it.

The Tmotor AK80-9 (depicted in Figure 7) was chosen as the optimal combination between torque output, volume, and weight. Motors in the AK series consist of a brushless DC motor, with an internal encoder and driver. This encoder was used in this implementation only to check the position of the motor. They offer position-only, speed-only, torque-only, and combination control. Control of the system is realized through five input variables: position,

Figure 7. The Tmotor AK80-9. On the left the unit as sold (with bolt inserted). On the right a unit with an additional coupling piece for attachment to the OSL gearbox input shaft.

velocity, feedforward torque, stiffness, and damping. The internal driver used the control loop depicted in Figure 8 to reach the desired states. The position and velocity are measured using the internal encoder.

For the initial control implementation, the impedance-based control used by Simon et al. [23] in the initial OSL clinical studies was chosen. Here minimum viable implementation required that only position, stiffness, and damping be controlled. Therefore, a position- and velocity-control was used on the Tmotor motor. The input variables were initially set according to biological lower limb data but can be tuned to get an idealized gait response as defined by the subject (or prosthetist).

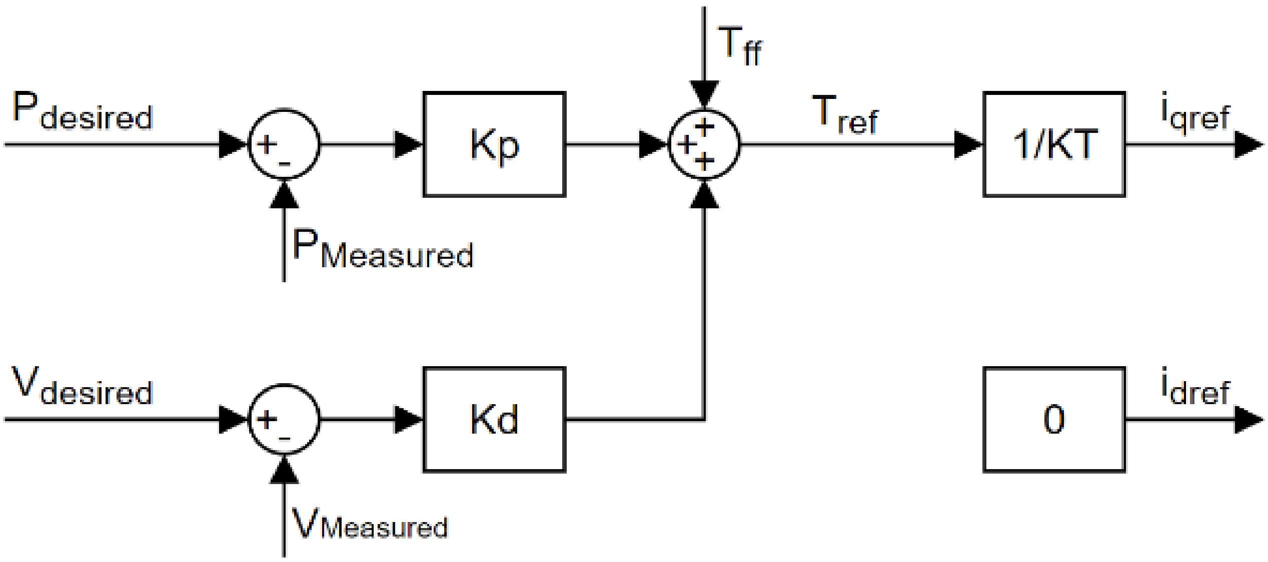

Figure 8. Motor control schematic

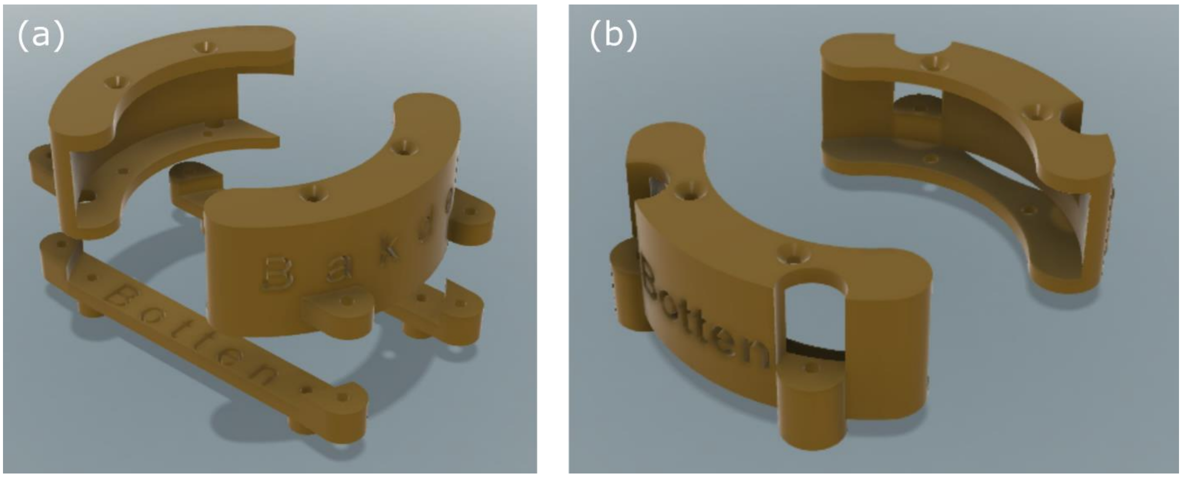

Figure 9. 3D printed motor cradles. (a) The ankle cradle (disassembled) (b) The knee cradle

To mount the new motors with minimal changes to the OSL body, a cradle for the motor was 3D printed in PLA (see Figure 9 for components and Figure 20 for full assembly). Additionally, to connect the motor drive shaft to the gearbox input shaft, a coupling was manufactured for the ankle and knee shafts. Because of the expected high torsion from rotation, this was milled out of aluminum (see right image of Figure 7).

The Tmotor motors have a position limit on all input variables. Only the position limitation conflicted with our range of moment requirements of the prosthesis. This prevented the motor from rotating outside of -12.5 and 12.5 radians from a set origin (as defined from the initial point the motor was turned on at). To move the actuated joints of the OSL through a full anatomical range this range must be increased. As this has yet to be implemented the ankle and knee joints were limited to 25° in this study. This is compared to the original design's 120° for the knee and 30° for the ankle.

State Machine

The OSL output divided the gait cycle into a multi-state format that controlled the response of the system based on the external data collected from the sensors. Figure 10 illustrates how the leg behavior responds to a pre-defined state until some threshold is met. The states are designed such that they divide the gait cycle into subdivisions. These subdivisions change the output variables according to prescribed functions and setpoints. In its final form, this system, called a "state machine", took a much more complex threshold system that used a larger pool of variables. The control system in this study used:

- Longitudinal force and mediolateral moment from the load cell
- Knee position and velocity from the knee encoder
- Ankle position from the ankle encoder
- Thigh angle from the IMU on the knee

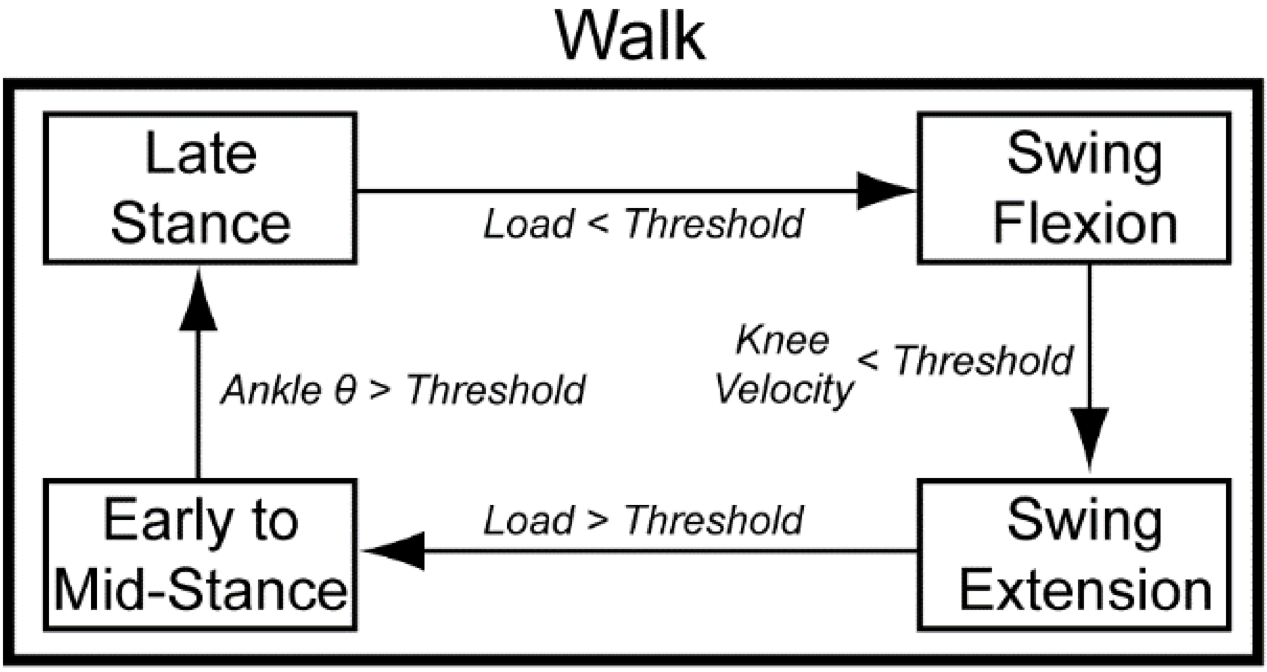

Figure 10 Simplified state machine. Licensed under CC BY 4.0 [23]

The sequence for the final state machine (similar to as shown in Figure 12) can be broken down into three functions. The nodes (blue boxes) define the behavior of the prosthesis until an event (orange boxes) is triggered which changes the node. These events are triggered when one or more of the sensors achieves some pre-defined value. The prosthesis' behavior to transition from one node to another (black arrows) is based on which event happens.

Foot Plate

The tested OSL model's foot section did not use the Össur LP Vari-Flex. It Instead, used a custom designed foot plate made of a similar carbon fiber (as seen in Figure 11). This foot plate was a flat plate and had very little elasticity. This change was made to simplify the response of the leg by removing an additional elastic variable for consideration.

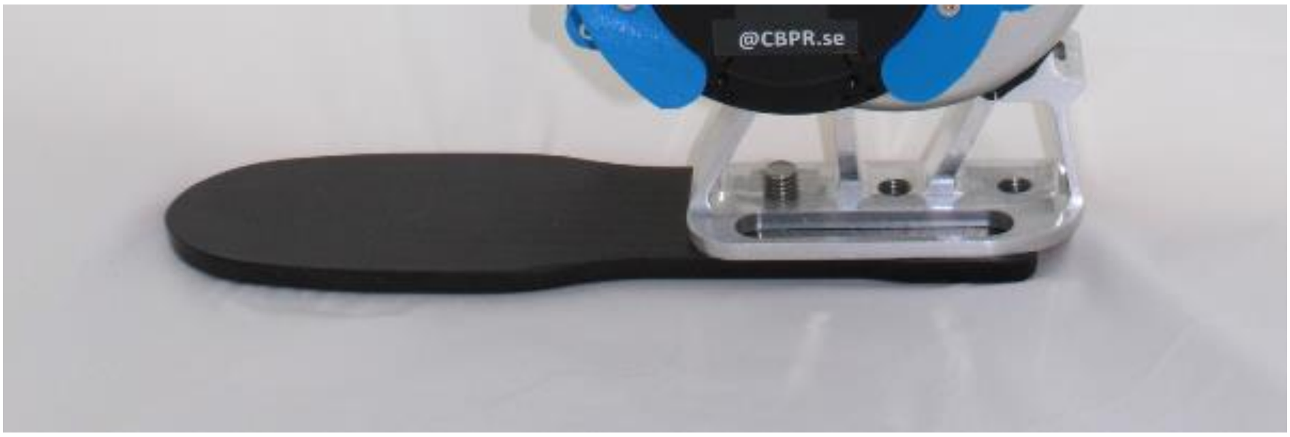

Figure 11. Carbon fiber flat foot

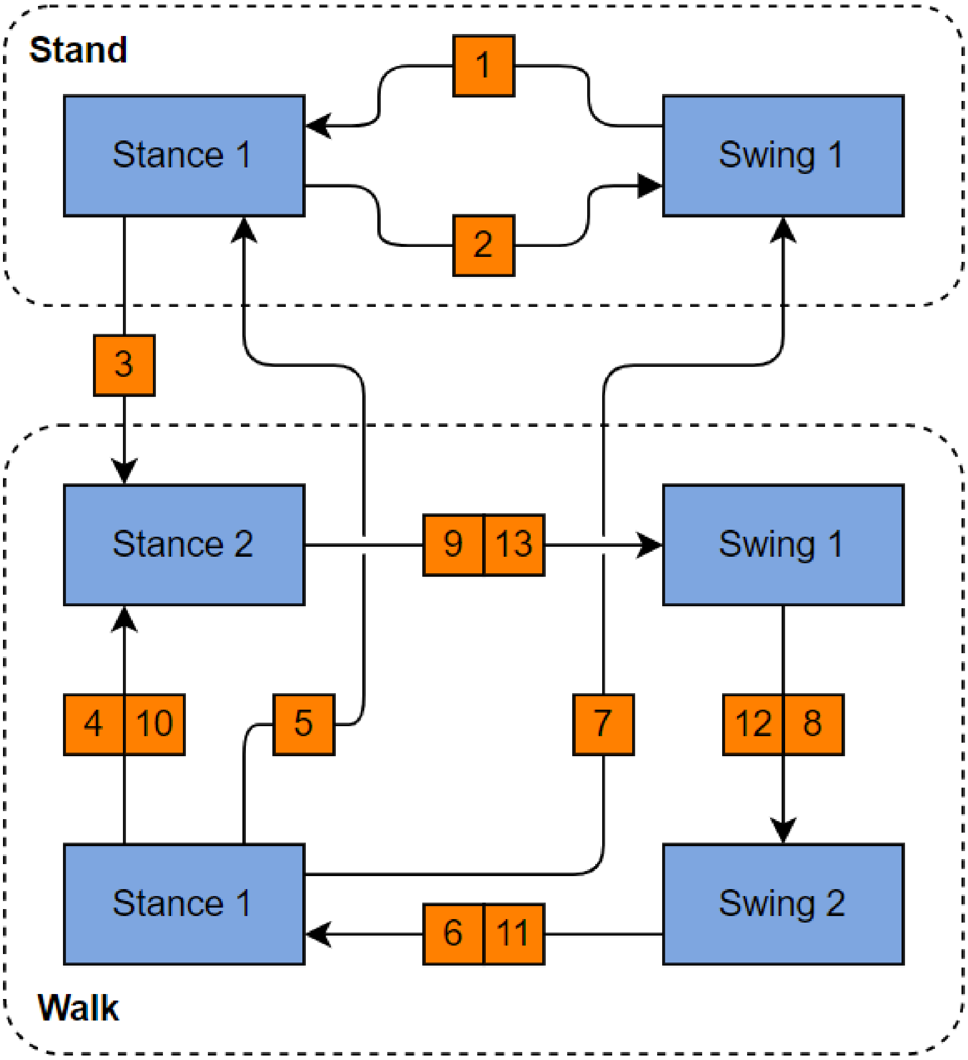

Figure 12. An example of a state machine with nodes (in blue) with multiple event sequences (in orange) that transition (black arrows) to different nodes.

Encoder

As with the previous design, the system used external absolute encoders (AS5048) mounted on the knee and ankle gearbox output axes (as seen in Figure 13). Unlike the internal encoder, this encoder would give the position of the driven sections (i.e. the position of the ankle and knee gearbox output shaft).

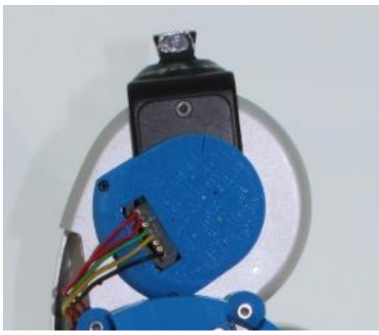
Figure 13. The encoder (with cover) as mounted on the knee gearbox output

Figure 14. IMU mounted on thigh segment of OSL

IMU

The ICM-20602, a six-axis (three-axis gyroscope, three-axis accelerometer) was chosen to replace the MPU-9250 nine-axis (three-axis gyroscope, three-axis accelerometer, three -axis magnetometer) used in the previous design because the magnetometer functionality was distorted by other electronics housed near it [24]. The MPU series has also been discontinued since the initial build of the OSL and therefore the ICM series was chosen. This device was previously integrated into the Dephy motor but was mounted separately for the Tmotor motor. In this iteration of the OSL the IMU was mounted to the thigh segment of the OSL and was used to derive the thigh angle (mounting shown in Figure 14). To compensate for drift a complementary filter was implemented using the thigh gyroscope and acceleration data to measure the change in thigh angle.

Osseointegration

Osseointegration allows direct skeletal attachment and bypasses the issues of soft tissue pressure and associated complications [25]. Research indicates that osseointegrated users who use their prosthesis more than 12 hours a day more than doubled from the same socket user group [2].

There are many types of osseointegrated implants, this study uses the Osseointegrated Prosthesis for the Rehabilitation of Amputees (OPRA) [26] (depicted in Figure 15). The bone-prosthesis interface consists of an implant (also called the fixture) which is completely embedded into the bone [2]. The distal end of this implant allows the mounting of a titanium rod, called

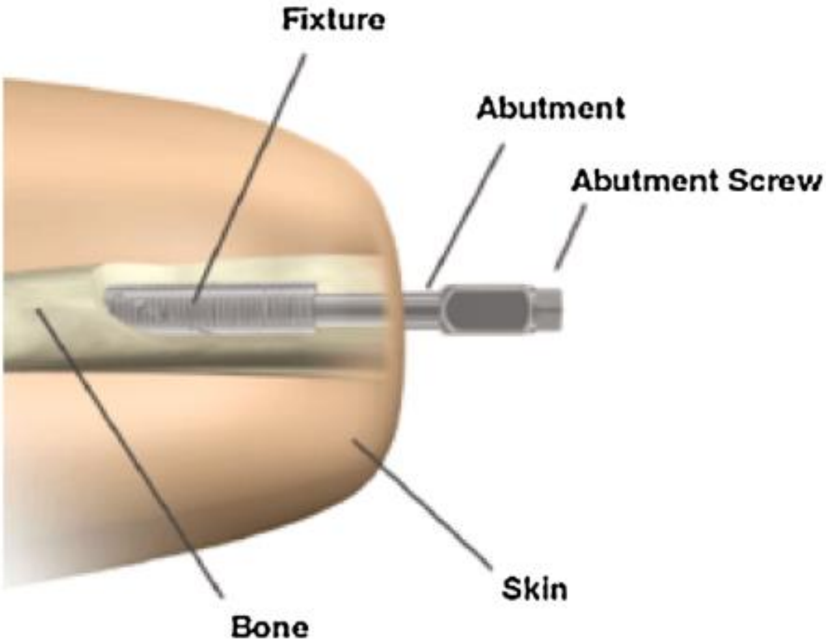

Figure 15. Osseointegrated interface, image courtesy of Integrum AB

the “abutment”, that extends through the skin. The abutment is press fit into the implant via the abutment screw.

Implanting a long bone with a metal implant can be considered a composite beam problem analytically. Therefore, in the sharing of forces the stiffer material will carry more of the load thereby unloading or ‘stress shielding’ the less stiff bone. Over time the adaptive nature of the biological tissue will mean that it resorbs and reduces in density [27]. The result could put the bone at risk in the event of high forces and therefore, a method of protecting the bone has been incorporated into the OPRA system: the abutment. The abutment is designed such that it

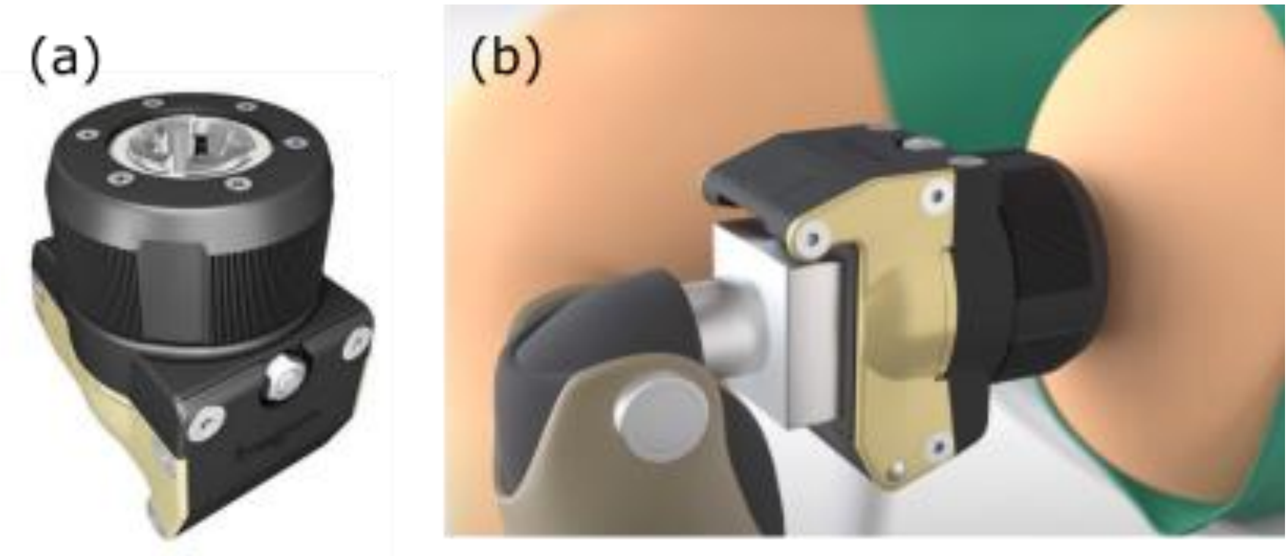

Figure 16. (a) The OPRA Axor II safety release system. (b) The OPRA Axor II as assembled between the prosthesis and the abutment. Images courtesy of Integrum AB

fractures before the fixture [27]. Additionally, a safety device separates the abutment and the prosthesis (as shown in Figure 16) to prevent direct damage to the abutment. Called the OPRA Axor II, the safety device is designed to detach when factory preset thresholds are exceeded in torsion or moment around the mediolateral axis.

Gait Cycle and Loading

Force Loads

The gait cycle can be broken down into stance and swing phases of leg motion (as shown in Figure 17) [28]. The stance phase acts like an inverted pendulum where the body rotates around the point at which the step began (the initial contact point). While this is happening, the opposing leg is swinging forward and above the ground to eventually contact the ground at a point ahead of the supporting (stance phase) leg. These roles alternate back and forth between each leg to form ambulation.

Gait analysis is comprised of kinematics and kinetics. Kinematics measure the motion of the concerned part(s) of the body (segments) usually via an optical camera system and biore-flective segment markers. Kinetics looks at the forces and moments of the segments of the body. Kinetic measurements can be obtained using embedded ground force plates or an instrumented treadmill [29] or a load cell built into the moving leg. In a gait lab the ground reaction forces (GRFs) measured by the force plates can be used to indirectly approximate the forces and mo-ments at the segment joint of interest via inverse kinematics. In this study the site of interest is the abutment, and an exact measurement of force and moment could be obtained using a load cell at the site of interest instead.

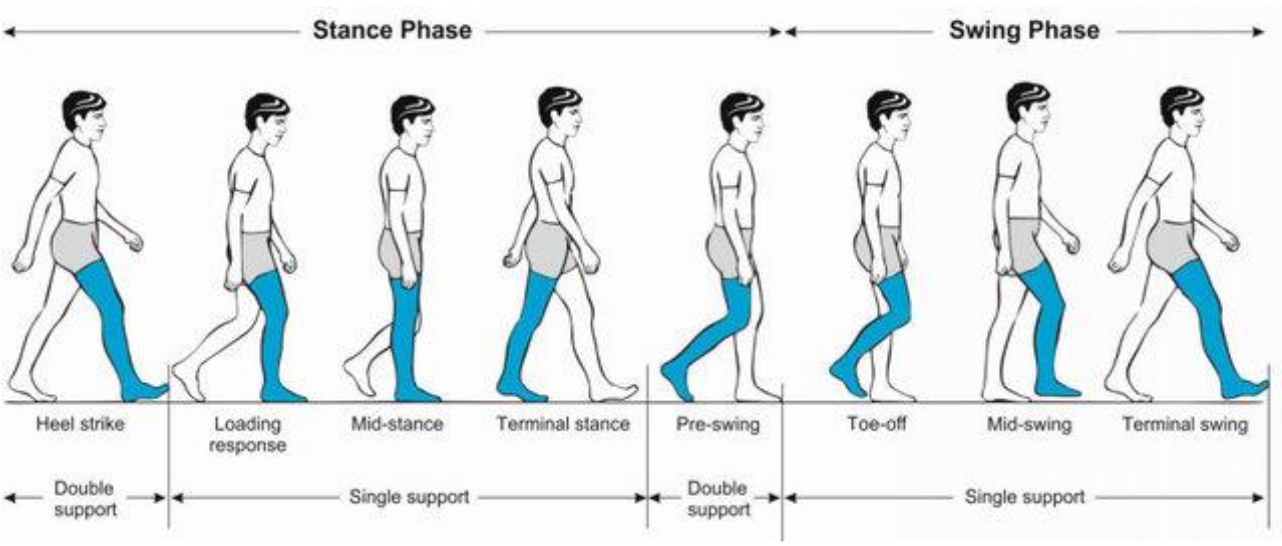

Figure 17. Phases of gait cycle. Licensed under CC BY 4.0 [28]

At the time of this writing there is no available literature on the force and moment loads experienced by the abutment of OPRA implants in users of ankle-knee active prostheses. This study sets out to answer this important research question. The approach will be to investigate non-amputated gait kinetics and transfemoral amputee gait kinetics from individuals using an OPRA fixture and a passive or semi active prostheses. Thereafter kinetics produced an effort to simulate gait using a quasi-static OSL gait cycle controlled by the onboard state machine in 'walk' mode can be compared.

Non-amputated Gait Kinetics

The closest approximation of the moment experience at the load cell of the prosthesis in this study for a non-amputee is the moment experienced by their knee. The GRFs are considered an acceptable analog to the load cell forces. As shown in Figure 18, in ambulation the vertical GRF is above zero (if positive is compression) during the stance phase [30]. From the initial contact of the heel until toe off there is an increase in GRF as weight is shifted onto one leg (initial loading phase). In the following period until heel rise, the GRF reduces due to the deceleration of the subject in the vertical direction. Once the heel begins rising, vertical GRF increases as a result of forward motion into the contralateral leg's initial contact and the push off provided by the plantar flexors. After this point the GRF reduces until zero as the weight is completely unloaded off the leg.

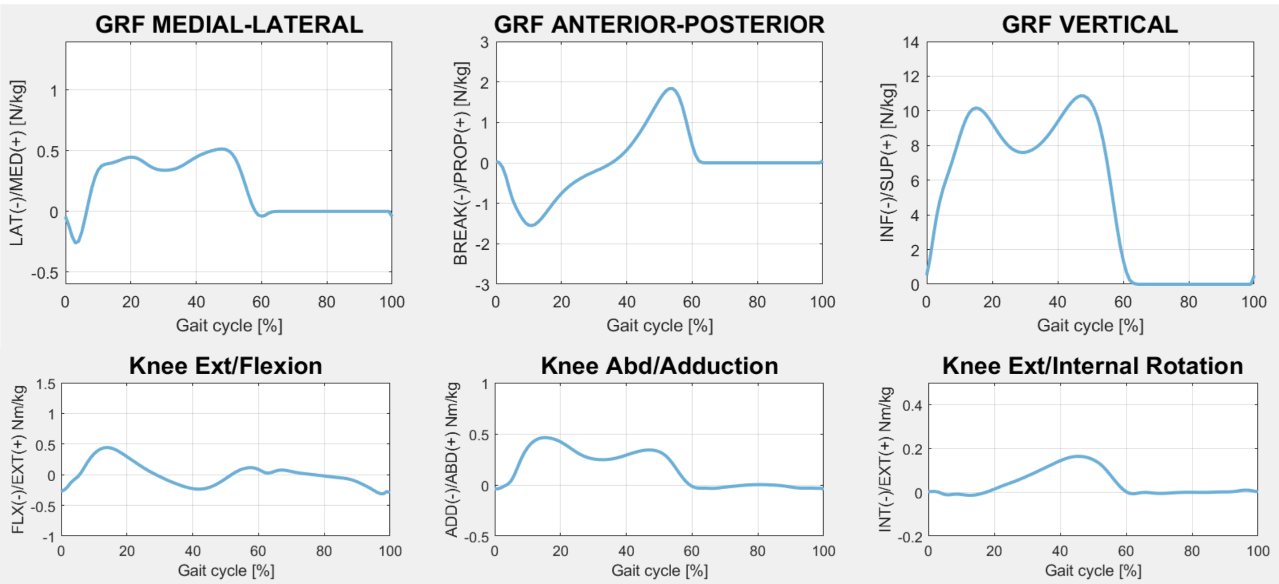

Figure 18. GRFs and the knee moments experience by non-amputee during level ground gaitThe black and thin line based off inverse kinematics. The shaded region is based off force plate data. Licensed under CC BY 4.0 [30].

In the anteroposterior (AP) plane, the anterior shear applied by the subject at heel strike causes an equal and opposite posterior GRF until midstance. Thereafter the shear becomes posteriorly applied by the subject and so an anterior GRF is observed.

The mediolateral forces are relatively smaller in magnitude with greater inter-subject variability [29]. The GRFs seen in this direction (mediolateral (ML) shear) are due to the changing center of mass of the body medially and therefore producing a lateral force causing an equal and opposite medial GRF.

Abutment Loads

The loads in osseointegrated abutments during ambulation as measured by a load cell have already been collected in existing literature for passive and semi-active prostheses. From Figure 19, we see that the shape of the force and moment graphs measured at the abutment are similar in shape to the average ground reaction forces in non-amputated subjects [31].

Aim

To determine the force and moment loads generated by the OSL on the OPRA abutment to ensure the moment around the ML axis falls beneath the threshold preset on the failsafe device (70Nm). To achieve this the OSL will be mounted to a single non-amputated subject via a prosthetic bypass socket. This study will only measure level ground ambulation. A successful design will ensure a ML moment <70 Nm.

Methods

The prosthesis was evaluated using the lower limb bypass socket that mounted to the user's leg. The 6-DOF College Park iPecs load cell was mounted between the distal end of the prosthesis and the proximal end of the bypass. The load cell center was located d=133 mm distal to the distal end of the fixture-abutment interface [3]. The load cell recorded the data at a frequency of 240 Hz.

The lower limb bypass was constructed from the iWalk leg crutch; the pedestal section was removed and replaced with standard prosthetic mountings (Figure 20a).

To compensate for the extra length added to the build by the load cell on one leg, the contralateral leg was raised with a shoe on a platform (depicted in Figure 20b).

The axes were set up such that positive directions were upward longitudinal, anterior, and lateral (as shown in Figure 20c). The moments about these followed the right hand rule.

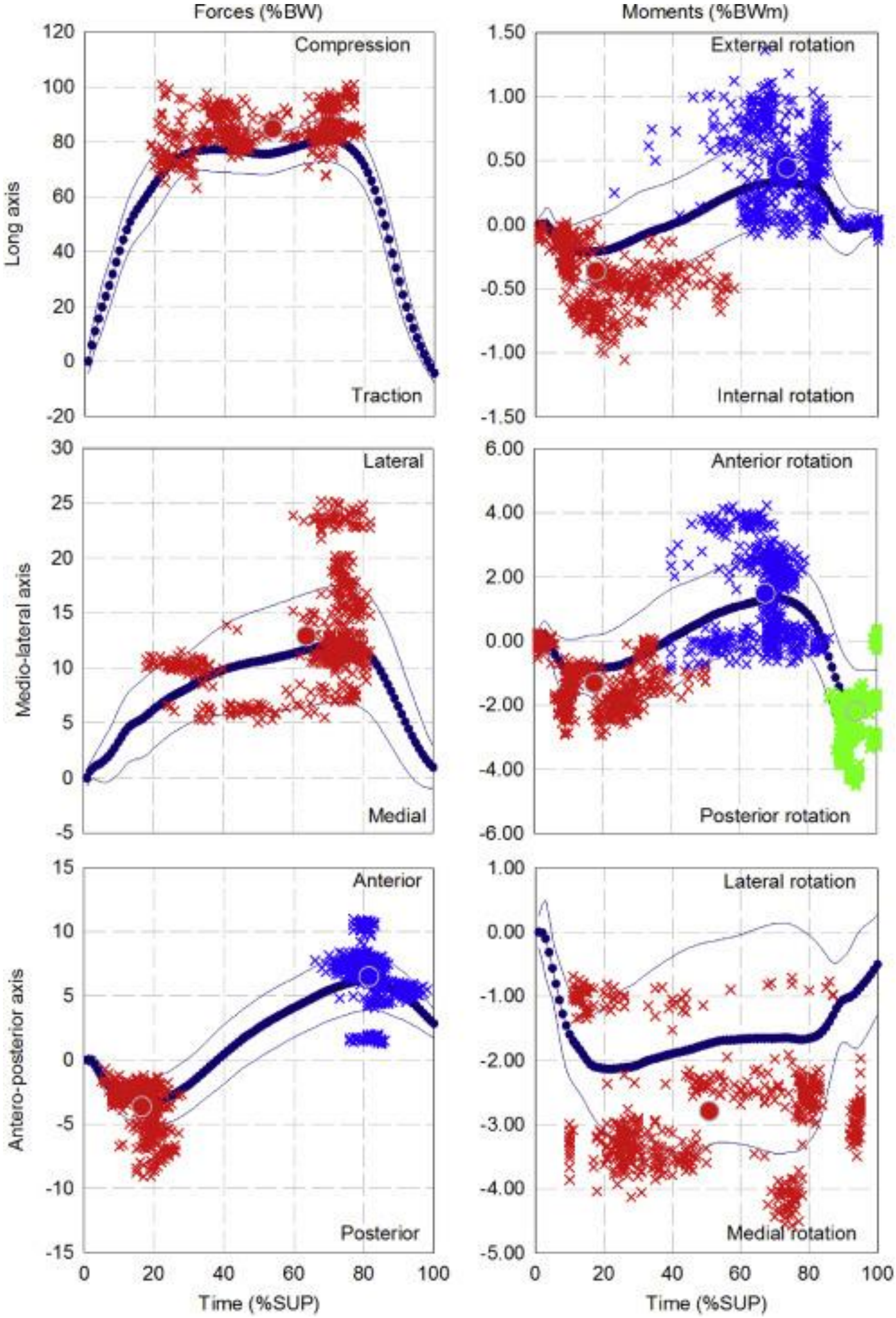

Figure 19. Normalized mean and standard deviation of forces and moments in abutment recorded from a load cell. Licensed under [CC BY-NC-ND 4.0](https://creativecommons.org/licenses/by-nc-nd/4.0/) [31]. Dispersion is depicted by crosses and mean by circles.

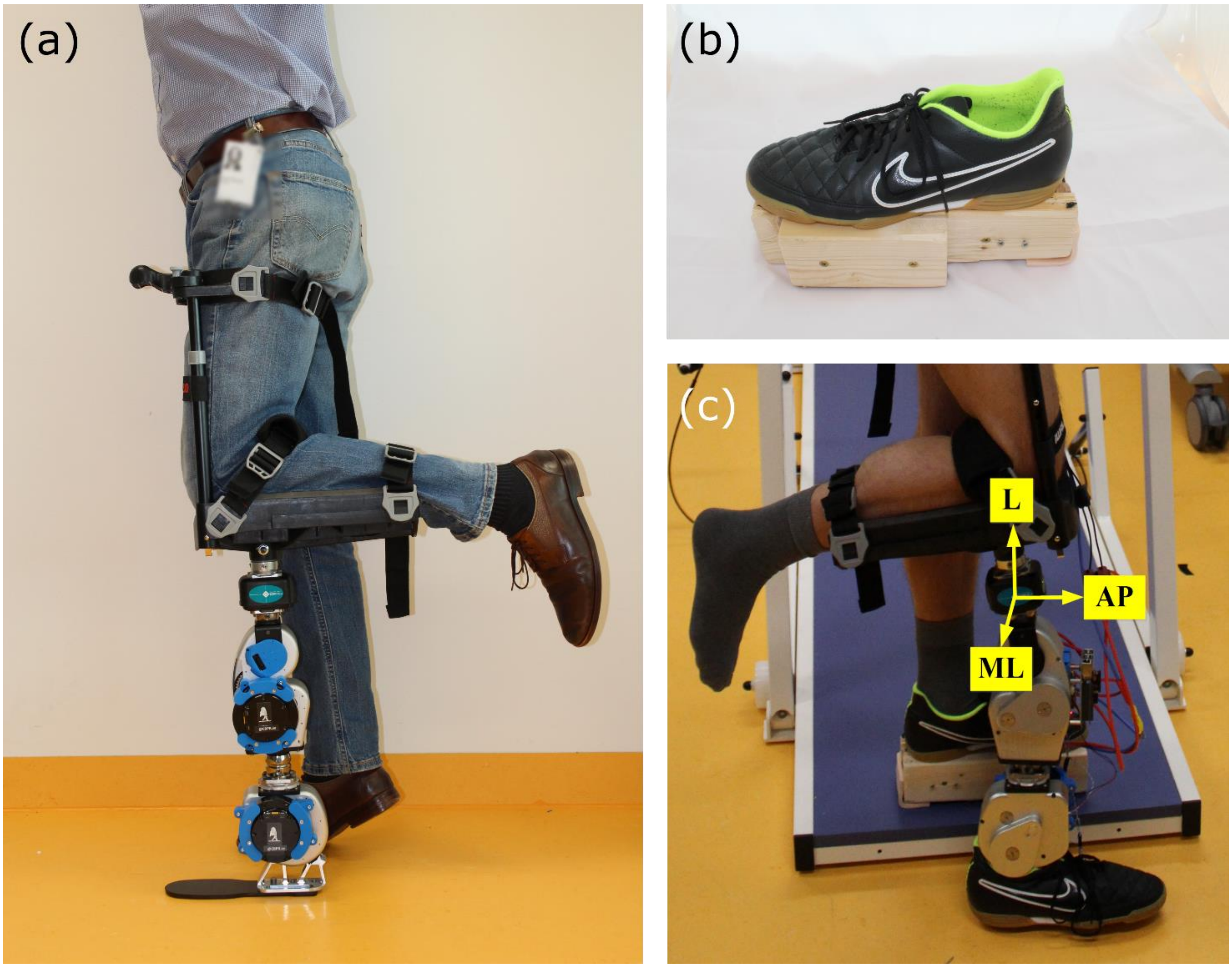

Figure 20. (a) iWalk with prosthesis mounted. (b) Shoe on platform. (c) Load cell coordinate system.

Tests used pre-recorded data to achieve the motor output, but the timing was adjusted as necessary for the users preferred speed and step length.

The user ambulated along a level parallel bar platform (as shown in Figure 21). The user was instructed to minimize the weight placed on the parallel bar.

Once the user was able to stand with the prosthesis, the ambulation program was started, and the user walked until consistent gait was achieved and was maintained for 2-3 minutes. Consistent gait was defined as having a defined heel strike and toe off and no dragging or stumbling.

Figure 21. Subject ambulating within parallel bars

Prior to recording, the load cell was zeroed with the prosthesis raised off the ground such that it was unloaded. Following this, the load cell began recording and the subject ambulated back and forth along the parallel bars. The observer was to mark in the load file every step that met the above definition of consistent.

The moment about the abutment was calculated according to the following equations:

$$M_{ML} = M_{ML,LC} + dF_{AP}$$

$$M_{AP} = M_{AP,LC} + dF_{ML}$$

Where M_{ML} and M_{AP} are the mediolateral and anteroposterior moments about the abutment. The $M_{ML,\,LC}$ and $M_{AP,\,LC}$ are the mediolateral and anteroposterior moments about the load cell.

Gait cycles were manually excised and pared down to gait cycles using the axial heel strike as the indicator of the cycle initiation.

Results

In addition to GRFs in established literature, the data will also be compared to the studies in Table II. All graphs are shown in percent of body weight. The user body weight was 77.0 kg.

Table II. Abutment load analysis studies

	Ankle		Knee	
	Propulsion	**Control**	**Propulsion**	**Control**
Lee et al. 2008 [32]	• Passive • Semi-active	• Passive	• Passive • Semi-active	• Passive • Adaptive
Frossard et al. 2013 [33]	• Passive	• Passive	• Passive • Semi-active	• Passive • Adaptive
Frossard 2019 [31]	• Passive	• Passive	• Passive • Semi-active	• Passive • Adaptive
Thesleff et al. 2020 [3]	• Passive • Semi-active	• Passive • Adaptive	• Passive • Semi-active	• Passive • Adaptive

Gait Cycle

In Figure 22 the double peak observed in non-amputated gait axial load curve was obtained in this study. However, the midstance dip was not as well defined, furthermore the phasing was different with maximum peaks at 28% and 33% of the gait cycle compared to 10% and 45% respectively.

In Figure 23, the anteroposterior curve obtained in this study was similar to amputee and non-amputee kinetics in distribution although the magnitude in the braking force (anterior shear) applied by the body was more than double that of the amputee data.

Figure 24 shows that the subject tends to drive the prosthesis medially during gait, this mirrors the non-amputee gait data but is opposite to amputee gait data from the study presented in Figure 19.

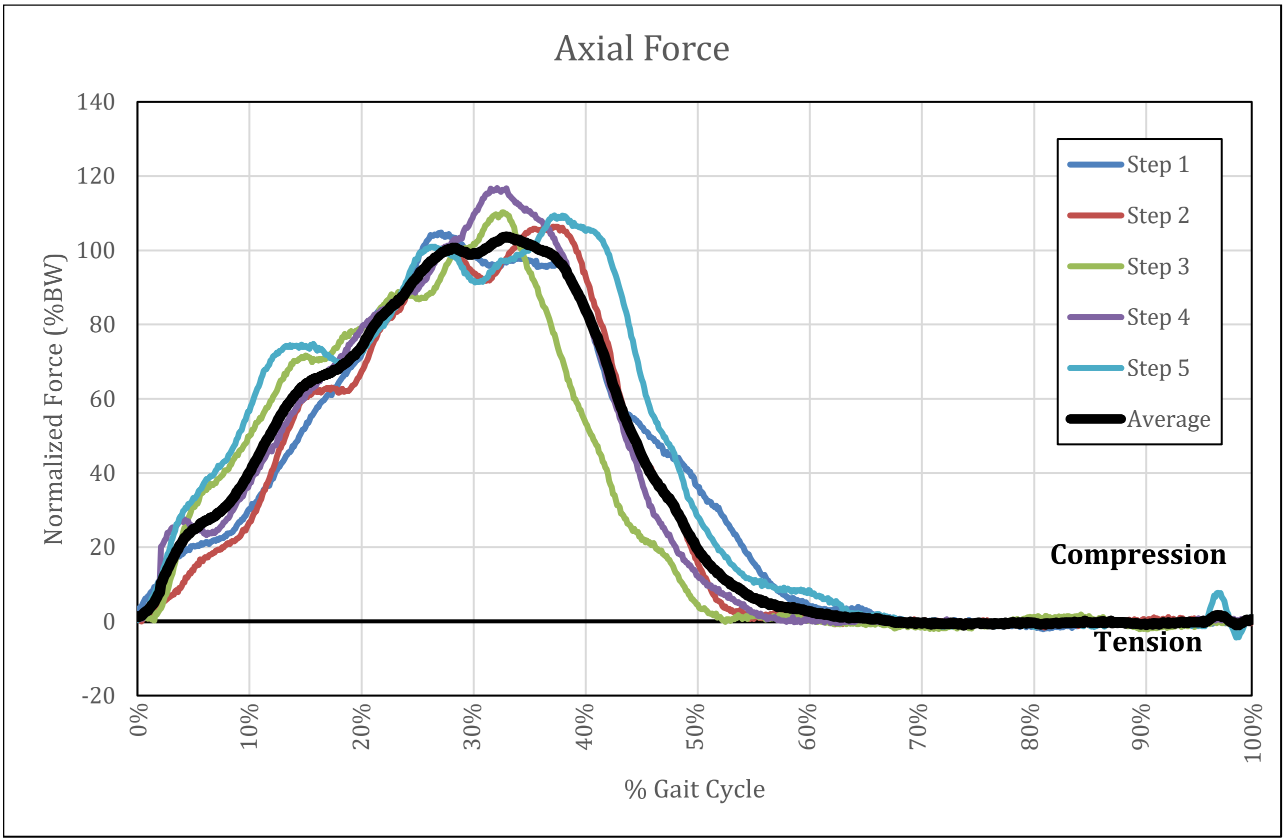

Figure 22. Normalized axial force

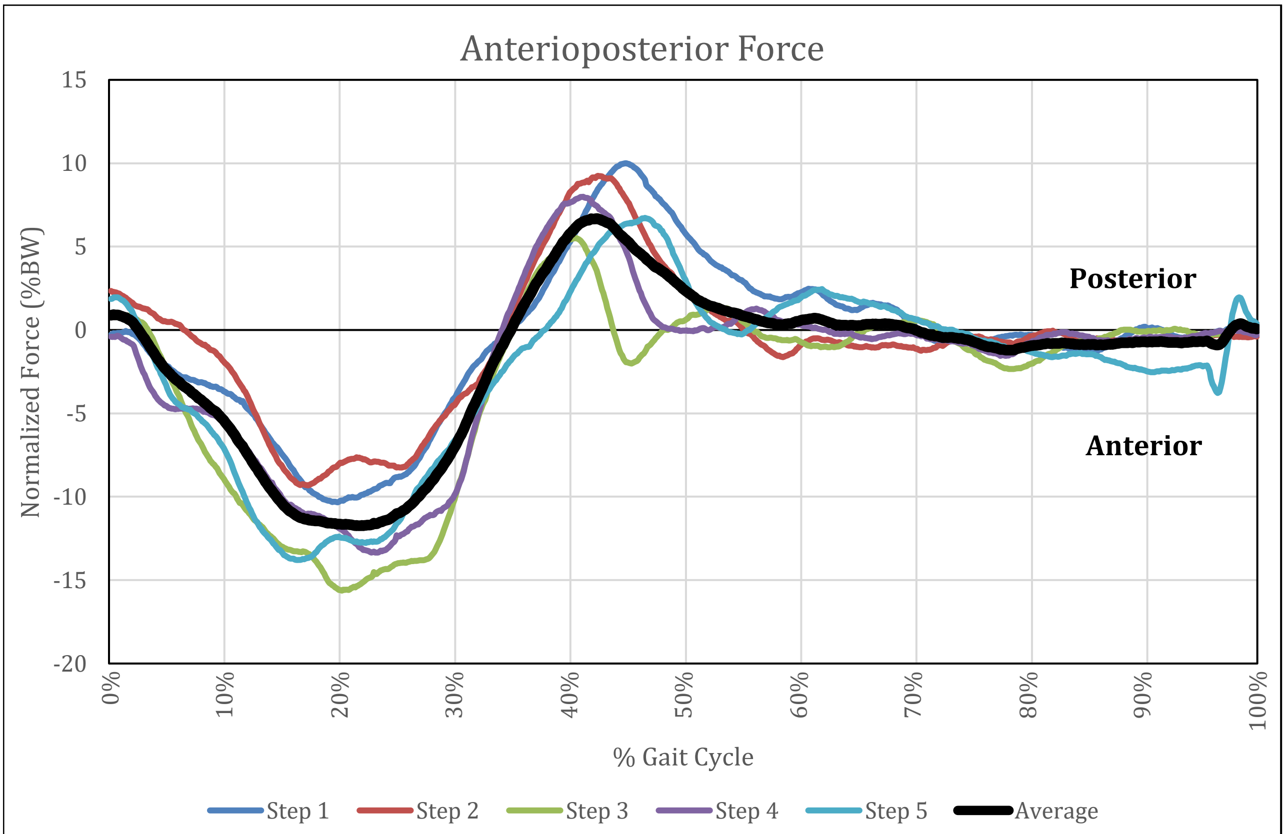

Figure 23. Normalized anteroposterior force

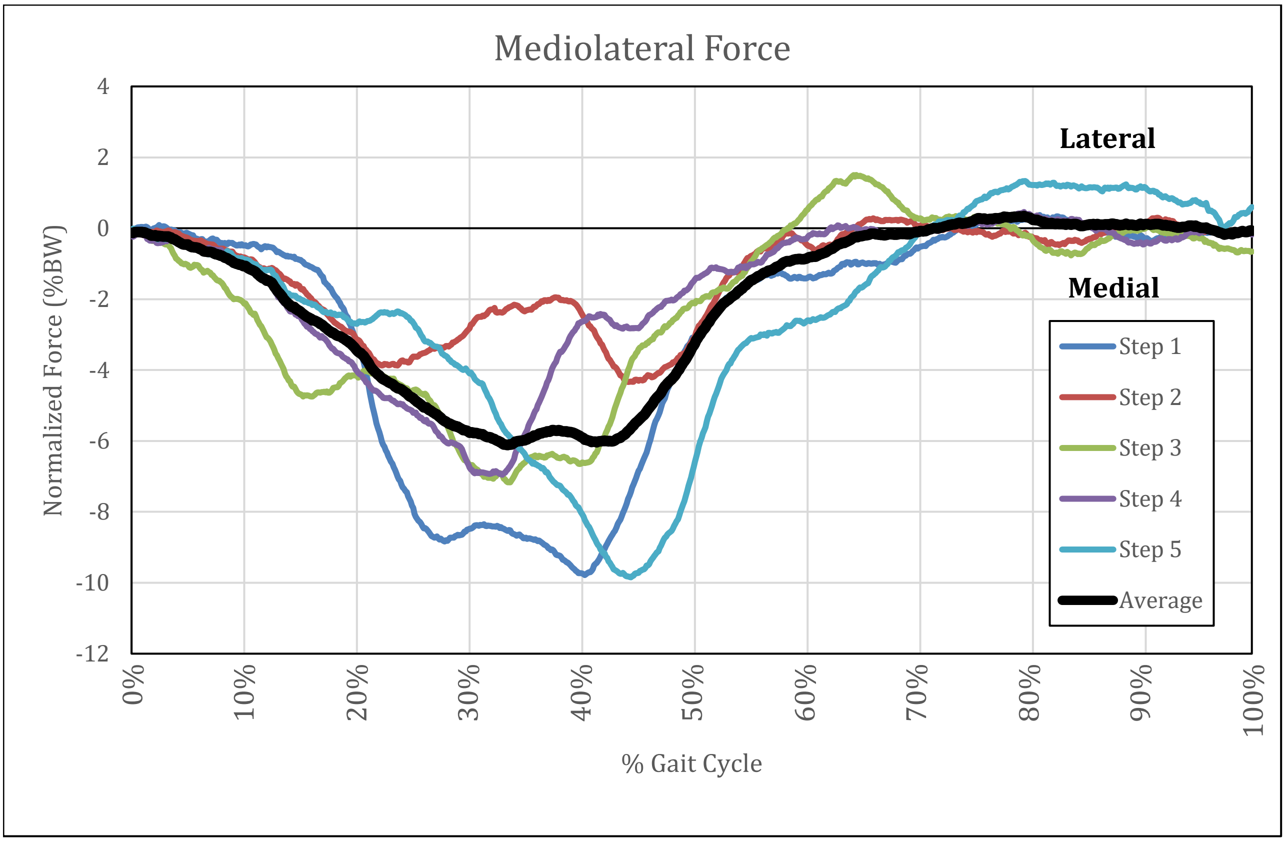

Figure 24. Normalized mediolateral force

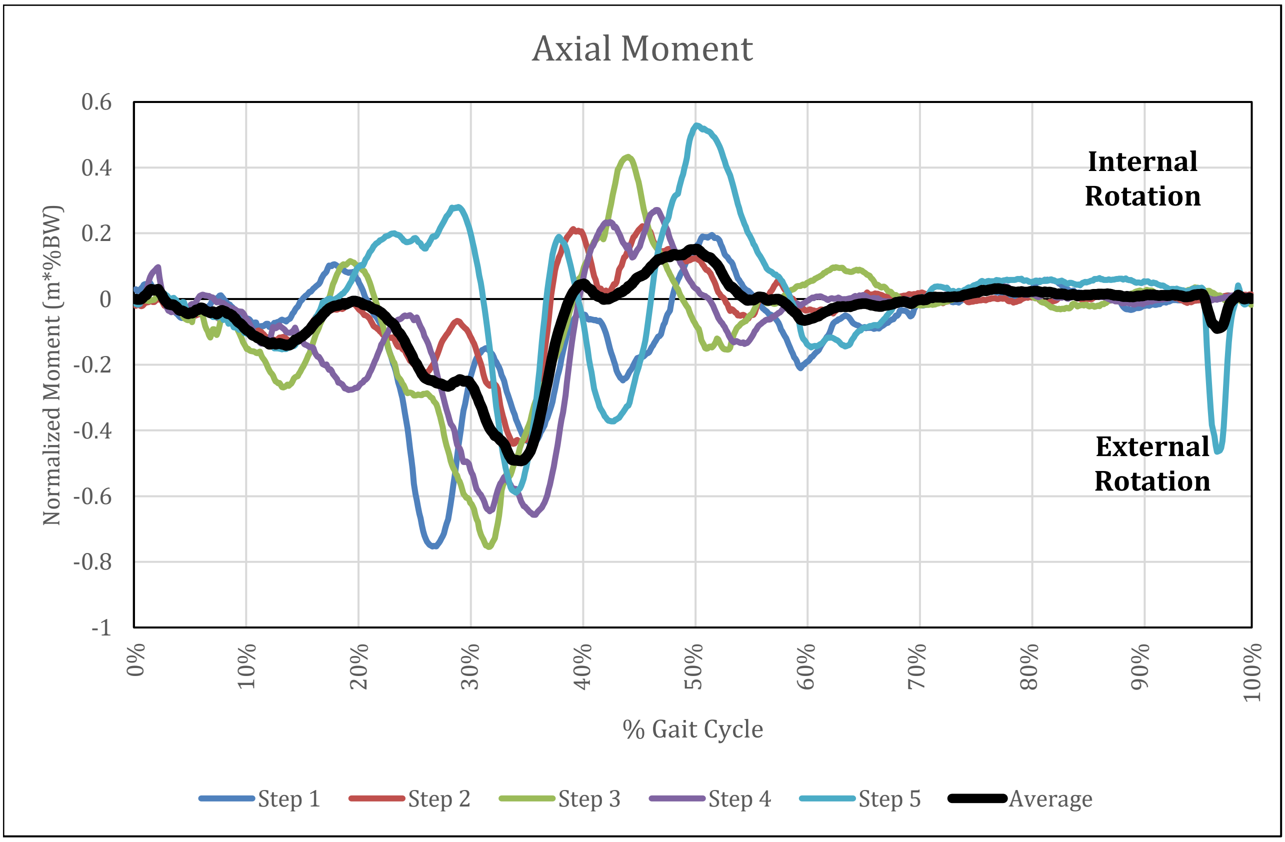

Figure 25. Normalized axial moment

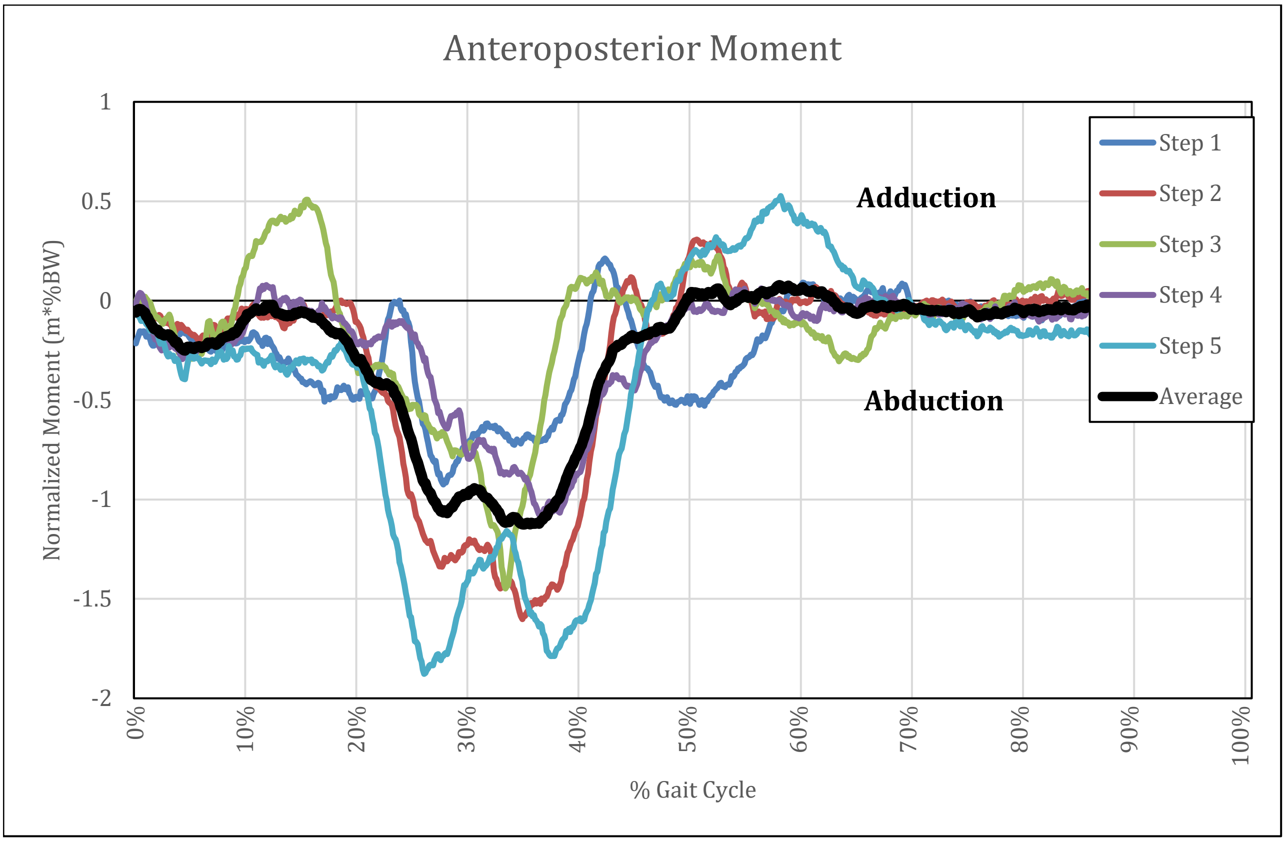

Figure 26. Normalized anteroposterior axis moment

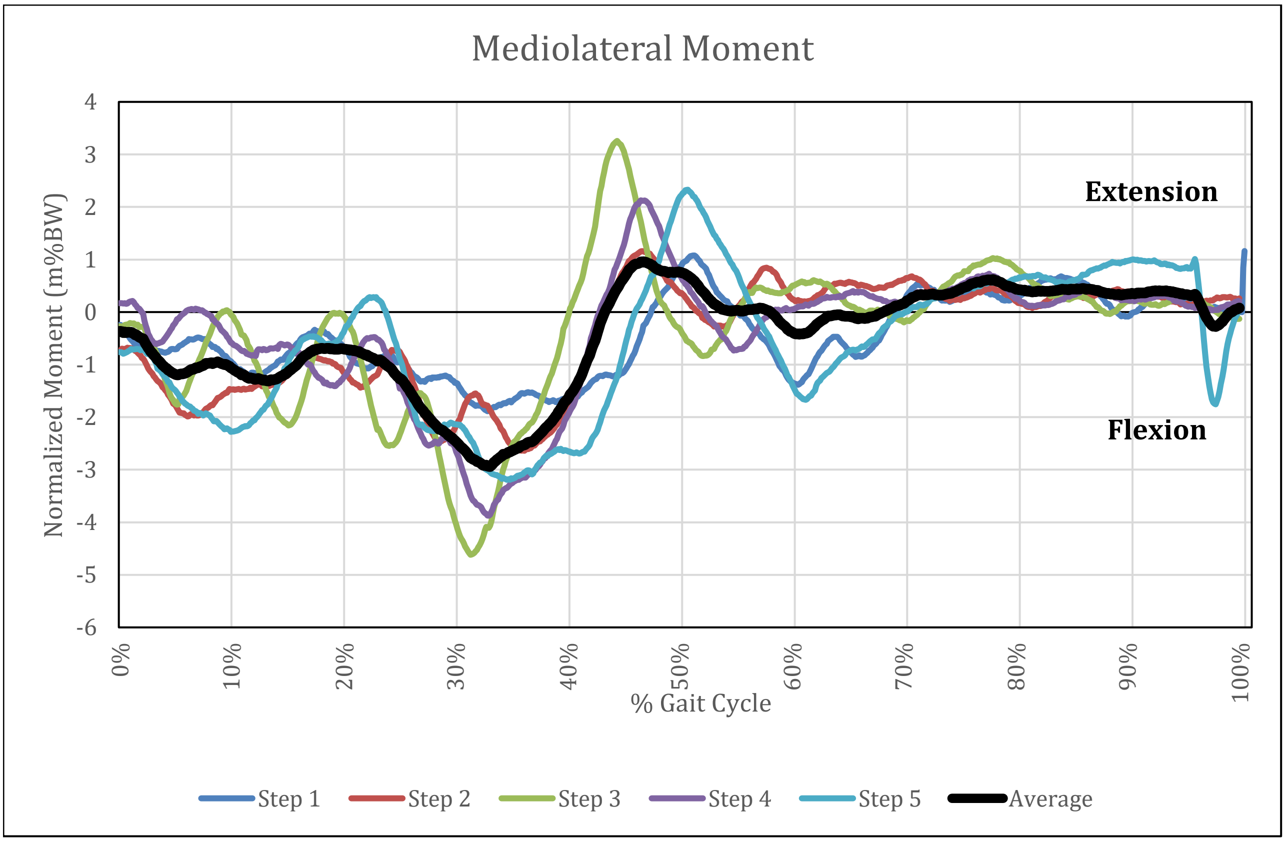

Figure 27. Normalized mediolateral axis moment

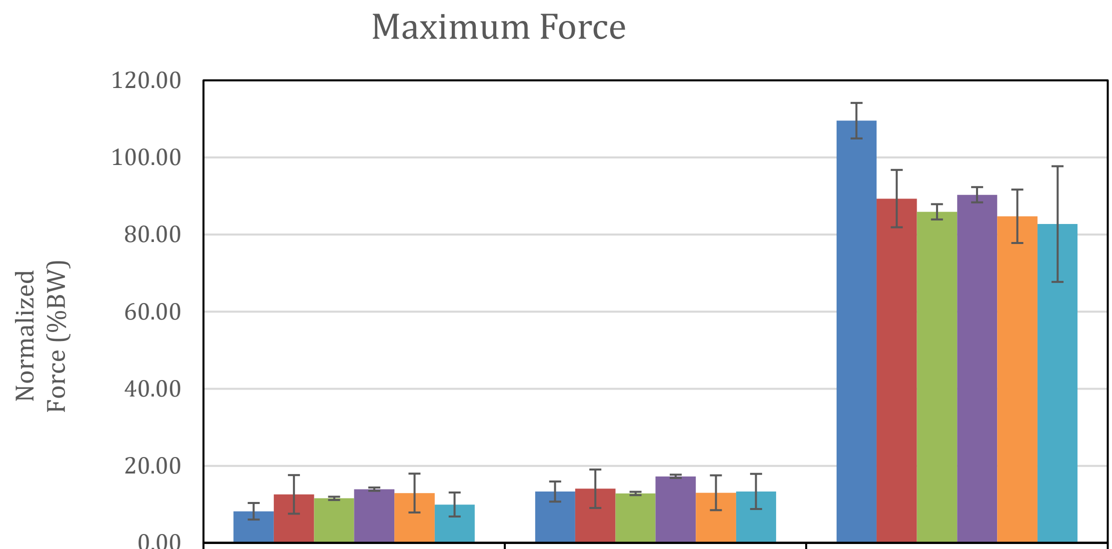

	ML	AP	L
Collected	8.20	13.31	109.53
Lee 2008	12.57	14.04	89.32
Frossard 2013 (Adaptive)	11.54	12.81	85.89
Frossard 2013 (SA)	13.93	17.26	90.32
Frossard 2019	12.92	13.00	84.73
Thesleff 2020	9.95	13.34	82.71

Figure 28. Normalized maximum force. SA = “semi-active”.

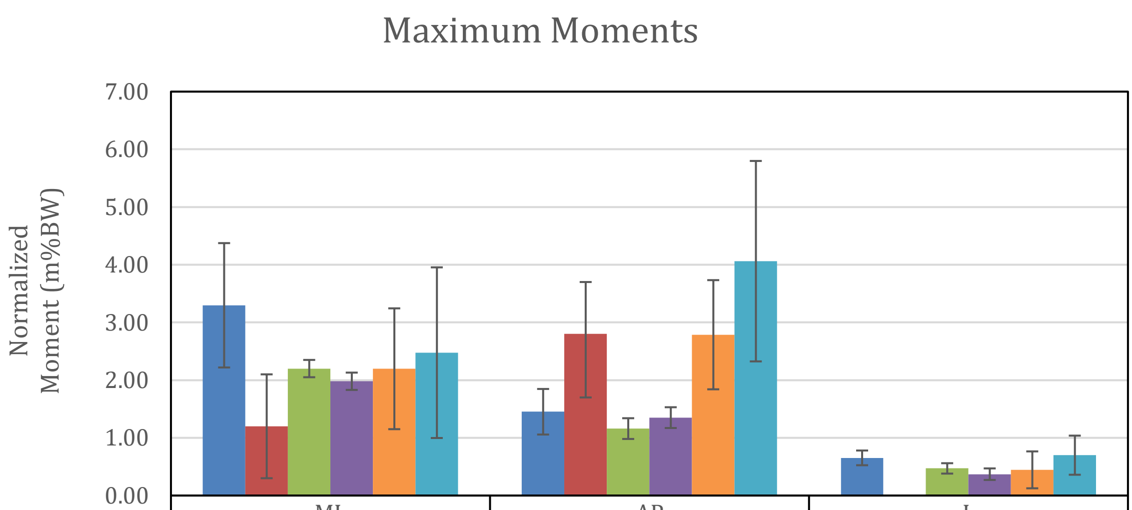

	ML	AP	L
Collected	3.30	1.45	0.65
Lee 2008	1.20	2.80	
Frossard 2013 (Adaptive)	2.20	1.16	0.47
Frossard 2013 (SA)	1.98	1.35	0.37
Frossard 2019	2.20	2.79	0.45
Thesleff 2020	2.48	4.06	0.70

Figure 29. Normalized maximum moment

Both the axial moment in Figure 25 and the anteroposterior moment in Figure 26 are similar in distribution to the study presented in Figure 19. However, the abduction peak from this study was nearly half the magnitude.

The average mediolateral moment in Figure 27 showed a flexion and return to zero. It was then followed by a small extension. This is a similar distribution to the amputee gait moment data from the study presented in Figure 19 although the peak magnitude is greater in flexion in this study compared to theirs.

Peak values

The maximum force and moment experienced at the abutment are depicted in Figure 28 and Figure 29, respectively.

Discussion

This study compared force and moment data to that obtained from transfemoral amputees using passive or semi-active prostheses in the existing literature. The data from the literature used a dynamic gait with a portable load cell and recorded continuous force and moment data. This study used quasi-static gait and recorded continuous force and moment data therefore some inconsistencies were expected in the comparison.

The OSL gait was inconsistent between steps. This stems from the limitations of the tuning tempo of the prosthesis of the user. Additionally, the length of the parallel bars would, even with successful ambulation, require stopping every three steps. Each step should therefore be considered as possibly both a standing to ambulating and ambulating to standing measure.

Force Loads

The axial forces collected in this study were similar but diverged slightly from reported literature. The reduced graph gradient may be a result of the stepping being initiated from a standing position and ending in a standing position instead of a more dynamic action. It could also be symptomatic of a limited knee range of motion or the altered biomechanics associated with a non-amputated subject using a bypass socket. Regardless of this, both the literature on abutment loads and the recorded data lacked the midstance dip likely due to the reduction in dynamic gait.

The anteroposterior force curves showed results similar in shape to the non-amputee and amputee literature. However, the maximum anterior peak value (braking force), was greater than subsequent posterior force peak (propulsion force). This difference will mean the subject will reduce in speed over time unless the contralateral leg produces a greater posterior shear to maintain constant speed. With so few steps taken and the steps not being dynamic in nature it was not possible to measure the speed of gait, furthermore asymmetries in gait are non-ideal [4].

Because of the natural variability of mediolateral forces and because those measured here are not outstanding, the prosthesis may not have had an impact in this plane [29]. Regardless, there was little difference between collected maximum magnitudes and other studies (8% less than the literature) and the distribution was very similar to what was found in Frossard et al. (2013) [33]

Moments

The axial moments are very similar to the published literature for both non-amputee and amputee subjects. The lower magnitude compared to other planes is to be expected given this has a smaller moment arm than the other axes [32].

The anteroposterior axis moment is similar in distribution to those in the amputee literature [31]–[33] and non-amputee data, barring a slow rate increase to the maximum moment. While Frossard et al. (2013) [33] was consistent in magnitude in measured moment, others were between two to three times larger [3], [31], [32]. In addition, the other literature is much larger in standard deviation with a value of more than double that of Lee et al [32] and more than quadrupled that of Thesleff et al. [3].

The mediolateral axis moment magnitude deviated from existing literature for amputee and non-amputee moments. For the latter, the initial extension is absent, however, this is consistent with amputee data. The mediolateral axis moment distribution was most similar to that in Lee et al., Frossard et al. (2013) and Frossard (2019). However, two differences are apparent: the first being the first maximum peak is about three times as large as the second maximum peak and it was observed ~5% earlier in the gait cycle. The first observation does not follow the mean trend line but is within the range of standard deviation. The second observation may suggest a different gait strategy even among amputees [32].

While being between 25-65% bigger in moment, the collected data proved to be well below the limit of the safety release. We see at an average value of 24.90 ± 8.14 [Nm], the mediolateral moment was below the threshold of 70 [Nm]. If data collected in this study accurately represents a transfemoral amputee, then it is unlikely that the user would reach the limit of the safety device in ambulation.

This is important because the safety release mechanism should not release in ambulation. It should only release when there is either the potential of abutment or bone fracture. If it were to release in everyday life it would cause the subject to stop moving immediately and to have to reconnect their prosthesis before they could continue. This may cause problems if for example they were walking quickly and were unable to stop immediately since it could cause a stumble or fall. Preventing unwanted disengagement of the safety device is paramount to its operation; conversely disengagement when required (for example in a fall) is an essential protection mechanism of any osseointegrated implant system. This study has demonstrated that the safety release device should not release under the normal conditions of walking, a further test may be to investigate whether the thresholds prescribed for release are suitable in the event of a fall and that it does disengage.

Limitations

Design

The original intention with the motor replacement was to do a simple swap of the motors on the existing system and translate the high level control as used in clinical studies into CAN communication. Unexpected delays meant reduced time to work on development and therefore requiring pre-programmed code to test the abutment loading. This requisited the quasi-static gait motion described earlier rather than a dynamic gait.

The motor position limit was similarly unexpected, with more time one solution could be to reduce the gearbox ratio to increase the range of motion. An alternative solution would be to use torque-only control of the motor. These could not be attempted here due to time constraints but should be feasible as the torque capabilities of the motor are well within the required torque values.

Testing

Data collection was undertaken in two one-hour sessions and the subject had very little time to acclimate to the prosthesis and had their contralateral leg increased in length by the wood block. In other studies, subjects had longer to familiarize themselves with the prosthesis (a year on average) and in order to generate comparable data this should be considered in further work.

To fully analyze the performance of the prosthesis, it is necessary to do kinematic analysis of the gait. This is particularly important when looking at compensatory motions in both legs. The motion of the hip and pelvis are difficult to determine based solely on kinetics, but they could have explained some of the gait cycle distribution that was seen.

The limited range of the motion of the knee motor made consistent ambulation difficult as the swing phase requires a bigger range. Therefore, it is unclear of how much of the gait was truly continuous or resetting step by step.

Furthermore, the results from this study were undertaken in a non-amputated individual who was an inexperienced user with different musculoskeletal anatomy compared to a trans-femoral amputee. In addition, the weight discrepancy of the leg, the knees height discrepancy and the posterior offset of the prosthetic bypass all contribute to population differences, that still need investigation.

Conclusion

An open-source prosthetic was modified to meet the higher demands of ambulation than the previous design could support. The result was a functioning ankle-knee prosthesis with an active propulsion and support system.

The loads on the abutment of an osseointegrated implant produced by this prosthesis were then measured. The maximum measured moment was within the ML moment limit of the safety device (Axor II). Assuming the non-amputee bypass user is a reasonable analog to an amputee, the OSL should be a viable prosthesis for the OPRA system.

References

[1] “Annual Report,” 2019. https://swedeamp.com/index.php/startsida/arsrapporter/.
[2] Integrum, “OPRA Implant System Instructions for Use,” *US Food Drug Adm.*, pp. 1–43, 2015.
[3] A. Thesleff, E. Haggstrom, R. Tranberg, R. Zugner, A. Palmquist, and M. Ortiz-Catalan, “Loads at the Implant-Prosthesis Interface During Free and Aided Ambulation in Osseointegrated Transfemoral Prostheses,” *IEEE Trans. Med. Robot. Bionics*, vol. 2, no. 3, pp. 497–505, Aug. 2020, doi: 10.1109/tmrb.2020.3002259.
[4] M. A. Price, P. Beckerle, and F. C. Sup, “Design Optimization in Lower Limb Prostheses: A Review,” *IEEE Trans. Neural Syst. Rehabil. Eng.*, vol. 27, no. 8, pp. 1574–1588, Aug. 2019, doi: 10.1109/TNSRE.2019.2927094.
[5] W. L. Childers and K. Z. Takahashi, “Increasing prosthetic foot energy return affects whole-body mechanics during walking on level ground and slopes,” *Sci. Rep.*, vol. 8, no. 1, p. 5354, Dec. 2018, doi: 10.1038/s41598-018-23705-8.
[6] R. Dedic and H. Dindo, “SmartLeg: An intelligent active robotic prosthesis for lower-limb amputees,” in *2011 XXIII International Symposium on Information, Communication and Automation Technologies*, Oct. 2011, pp. 1–7, doi: 10.1109/ICAT.2011.6102090.
[7] D. Johansen, C. Cipriani, D. B. Popovic, and L. N. S. A. Struijk, “Control of a Robotic Hand Using a Tongue Control System-A Prosthesis Application,” *IEEE Trans. Biomed. Eng.*, vol. 63, no. 7, pp. 1368–1376, 2016, doi: 10.1109/TBME.2016.2517742.
[8] D. S. Pieringer, M. Grimmer, M. F. Russold, and R. Riener, “Review of the actuators of active knee prostheses and their target design outputs for activities of daily living,” in *2017 International Conference on Rehabilitation Robotics (ICORR)*, Jul. 2017, pp. 1246–1253, doi: 10.1109/ICORR.2017.8009420.
[9] P. Malcolm, R. E. Quesada, J. M. Caputo, and S. H. Collins, “The influence of push-off timing in a robotic ankle-foot prosthesis on the energetics and mechanics of walking,” *J. Neuroeng. Rehabil.*, vol. 12, no. 1, p. 21, Dec. 2015, doi: 10.1186/s12984-015-0014-8.
[10] J. M. Caputo and S. H. Collins, “Prosthetic ankle push-off work reduces metabolic rate but not collision work in non-amputee walking,” *Sci. Rep.*, vol. 4, no. 1, p. 7213, May 2015, doi: 10.1038/srep07213.
[11] B. J. Hafner and R. L. Askew, “Physical performance and self-report outcomes associated with use of passive, adaptive, and active prosthetic knees in persons with unilateral, transfemoral amputation: Randomized crossover trial,” *J. Rehabil. Res. Dev.*, vol. 52, no. 6, pp. 677–700, 2015, doi: 10.1682/JRRD.2014.09.0210.
[12] E. J. Wolf, V. Q. Everding, A. A. Linberg, J. M. Czerniecki, and C. J. M. Gambel, “Comparison of the Power Knee and C-Leg during step-up and sit-to-stand tasks,” *Gait Posture*, vol. 38, no. 3, pp. 397–402, Jul. 2013, doi: 10.1016/j.gaitpost.2013.01.007.
[13] “EmPOWERing Active Seniors With Energy - Full Text View - ClinicalTrials.gov.” https://clinicaltrials.gov/ct2/show/study/NCT02958553 (accessed Oct. 21, 2020).
[14] D. H. Gates, J. M. Aldridge, and J. M. Wilken, “Kinematic comparison of walking on uneven ground using powered and unpowered prostheses,” *Clin. Biomech.*, vol. 28, no. 4, pp. 467–472, Apr. 2013, doi: 10.1016/j.clinbiomech.2013.03.005.
[15] B. E. Lawson, J. Mitchell, D. Truex, A. Shultz, E. Ledoux, and M. Goldfarb, “A Robotic Leg Prosthesis: Design, Control, and Implementation,” *IEEE Robot. Autom. Mag.*, vol. 21, no. 4, pp. 70–81, Dec. 2014, doi: 10.1109/MRA.2014.2360303.
[16] L. Flynn, J. Geeroms, R. Jimenez-Fabian, B. Vanderborght, N. Vitiello, and D. Lefeber, “Ankle–knee prosthesis with active ankle and energy transfer: Development of the CYBERLEGs Alpha-Prosthesis,” *Rob. Auton. Syst.*, vol. 73, pp. 4–15, Nov. 2015, doi: 10.1016/j.robot.2014.12.013.
[17] M. Wu, T. Driver, S.-K. Wu, and X. Shen, “Design and Preliminary Testing of a Pneumatic Muscle-Actuated Transfemoral Prosthesis,” *J. Med. Device.*, vol. 8, no. 4, pp. 1–7, Dec. 2014, doi: 10.1115/1.4026830.
[18] J. Mendez, S. Hood, A. Gunnel, and T. Lenzi, “Powered knee and ankle prosthesis with indirect volitional swing control enables level-ground walking and crossing over obstacles,” *Sci. Robot.*, vol. 5, no. 44, p. eaba6635, Jul. 2020, doi: 10.1126/scirobotics.aba6635.

[19] T. Elery, S. Rezazadeh, C. Nesler, and R. D. Gregg, “Design and Validation of a Powered Knee–Ankle Prosthesis With High-Torque, Low-Impedance Actuators,” *IEEE Trans. Robot.*, vol. 36, no. 6, pp. 1649–1668, Dec. 2020, doi: 10.1109/TRO.2020.3005533.
[20] A. F. Azocar, L. M. Mooney, J. F. Duval, A. M. Simon, L. J. Hargrove, and E. J. Rouse, “Design and clinical implementation of an open-source bionic leg,” *Nat. Biomed. Eng.*, vol. 4, no. 10, pp. 941–953, Oct. 2020, doi: 10.1038/s41551-020-00619-3.
[21] E. J. Rouse, “Open-Source Leg,” 2021. https://opensourceleg.com/ (accessed Sep. 06, 2021).
[22] “Peak Current vs Continuous/Rated Current | Tutorials of Cytron Technologies.” https://tutorial.cytron.io/2016/12/01/peak-current-vs-continuousrated-current/ (accessed Sep. 19, 2021).
[23] A. M. Simon *et al.*, “Configuring a powered knee and ankle prosthesis for transfemoral amputees within five specific ambulation modes,” *PLoS One*, vol. 9, no. 6, 2014, doi: 10.1371/journal.pone.0099387.
[24] “dephyactpack02 [FlexSEA Wiki].” https://dephy.com/wiki/flexsea/doku.php?id=dephyactpack02 (accessed Oct. 04, 2021).
[25] R. S. Jayesh and V. Dhinakarsamy, “Osseointegration,” *Journal of Pharmacy and Bioallied Sciences*, vol. 7, no. 5. Wolters Kluwer -- Medknow Publications, pp. S226–S229, Apr. 01, 2015, doi: 10.4103/0975-7406.155917.
[26] A. Thesleff, R. Brånemark, B. Håkansson, and M. Ortiz-Catalan, “Biomechanical Characterisation of Bone-anchored Implant Systems for Amputation Limb Prostheses: A Systematic Review,” *Ann. Biomed. Eng.*, vol. 46, no. 3, pp. 377–391, Mar. 2018, doi: 10.1007/s10439-017-1976-4.
[27] P. Stenlund, M. Trobos, J. Lausmaa, R. Brånemark, P. Thomsen, and A. Palmquist, “Effect of load on the bone around bone-anchored amputation prostheses,” *J. Orthop. Res.*, vol. 35, no. 5, pp. 1113–1122, May 2017, doi: 10.1002/jor.23352.
[28] W. Pirker and R. Katzenschlager, “Gait disorders in adults and the elderly,” *Wien. Klin. Wochenschr.*, vol. 129, no. 3–4, pp. 81–95, Feb. 2017, doi: 10.1007/s00508-016-1096-4.
[29] D. A. Neumann, “Kinesiology of the Musculoskeletal System (PDFDrive).pdf.” p. 784, 2002.
[30] C. A. Fukuchi, R. K. Fukuchi, and M. Duarte, “A public dataset of overground and treadmill walking kinematics and kinetics in healthy individuals,” *PeerJ*, vol. 6, no. 4, p. e4640, Apr. 2018, doi: 10.7717/PEERJ.4640.
[31] L. Frossard, “Loading characteristics data applied on osseointegrated implant by transfemoral bone-anchored prostheses fitted with basic components during daily activities,” *Data Br.*, vol. 26, p. 104492, Oct. 2019, doi: 10.1016/j.dib.2019.104492.
[32] W. C. C. Lee *et al.*, “Magnitude and variability of loading on the osseointegrated implant of transfemoral amputees during walking,” *Med. Eng. Phys.*, vol. 30, no. 7, pp. 825–833, Sep. 2008, doi: 10.1016/j.medengphy.2007.09.003.
[33] L. Frossard, E. Häggström, K. Hagberg, and R. Brånemark, “Load applied on bone-anchored transfemoral prosthesis: Characterization of a prosthesis-A pilot study,” *J. Rehabil. Res. Dev.*, vol. 50, no. 5, pp. 619–634, 2013, doi: 10.1682/JRRD.2012.04.0062.

DEPARTMENT OF ELECTRICAL ENGINEERING
CHALMERS UNIVERSITY OF TECHNOLOGY
Gothenburg, Sweden 2021
www.chalmers.se

CHALMERS
UNIVERSITY OF TECHNOLOGY